Simulation of the structure of amorphous silicon dioxide

Lester Guttman and Shafiqur M. Rahman*
Materials Science Division, Argonne National Laboratory, Argonne, Illinois 60439
(Received 14 July 1987)

Computer models of amorphous silicon dioxide have been generated by systematic procedures. The models are all stoichiometric, perfectly coordinated and periodic, and composed of SiO_4 tetrahedra sharing corners to form a random network. Starting from various random arrangements, each example is subjected to a series of modifications of its connectivity which reduce its potential energy under a valence-force type of potential function. Several examples have been constructed for each of four choices of starting point and method of connectivity modification. The number of silicon atoms in the repeating unit has been varied from 30 to 108, with twice as many oxygen atoms. The force constants have been chosen by comparison with experiment of the computed density and elastic moduli. The calculated neutron scattering of many of the examples is in excellent agreement with recent experiments of high precision. However, examples containing rings of three or four tetrahedra show scattering at small momentum transfer which deviates increasingly from experiment as the numbers of these rings increase.

I. INTRODUCTION

Amorphous silica is, from several viewpoints, so important as to justify the many attempts that have been made to account for its properties at a fundamental level. Glassy SiO_2 is invariably obtained on cooling from the melt, and the product is well-characterized provided precautions are taken, especially to exclude water. Mixtures of SiO_2 with other oxides are the most common commercial glasses, and the oxidation of silicon yields amorphous insulating films that now dominate the semiconducting-device industry. Although the uses of these glasses can hardly be said to have been retarded by our ignorance of their atomic structures, it is true that the atomic structure of amorphous silica (a-SiO_2) is still controversial. The reason for this situation, which would not have persisted this long for a crystalline material of similar complexity, stems from the nature of noncrystalline solids. The concept of "atomic structure" ordinarily means specification of the relative positions of the constituent atoms to arbitrarily large distances, information which can be derived in principle from diffraction measurements on crystals. Such a measurement always yields only a pair-distribution function, which, combined with the periodicity condition, is sufficient to define the atomic structure in the usual sense for a crystal. For a glass, diffraction data alone are insufficient to define the structure, even if only a single element is present, and if there are two or more components, as in SiO_2, several independent diffraction measurements are needed to determine even the pair-distribution functions.

We have recalled these well-known facts in order to lay the groundwork for our method of attacking the structural problem, which is to test our structural models primarily by comparison of their calculated structure factors directly with diffraction data. We regard this procedure as subject to fewer untestable assumptions than the customary comparison of calculated and "observed" real-space radial distribution functions (RDFs), and equally as precise computationally. However, because features of the structure factor are not uniquely associated with particular structural features, we have also made use of calculated RDFs for secondary comparisons.

Earlier studies of this kind have largely been confined to hand-built models. To draw accurate conclusions from such models, it is necessary at least to simulate them by computer and to determine the atomic positions by relaxation under a well-defined potential. This has been done by Gaskell and Tarrant[1] for the Bell-Dean model and by Evans, Gaskell, and Nex[2] for four models of SiO_2 derived from previously constructed models of amorphous silicon. However, as remarked by these authors, the results for these or any other finite model are subject to serious surface effects which are difficult to estimate. We have adopted the accepted remedy for this problem, which is to use periodic boundary conditions. The absence of free surfaces presumably reduces the size effects greatly, and upper bounds to the residual effects can perhaps be estimated from the variations of properties as the size of the repeating unit is changed by a large factor.

II. CONSTRUCTION OF MODELS

We have assumed, with the majority of workers in the field, that a-SiO_2 is made up of SiO_4 tetrahedra sharing corners, the whole constituting a continuous (nearly) random network. Then the Si atoms are perfectly fourfold-coordinated to oxygen and the O atoms twofold-coordinated to Si. As others have noted, the Si

 ©1988 The American Physical Society

atoms themselves form a four-coordinated random network. Therefore it is possible to generate a topologically acceptable model of a-SiO_2 from a model of amorphous silicon (a-Si) simply by inserting an oxygen atom between every pair of Si atoms. All of our models have begun as perfectly four-coordinated nets of Si atoms, but have followed different paths in their later development. In all cases, the Si networks made by any quasirandom process are not acceptable as realistic models of a-Si, nor are they acceptable as models of a-SiO_2 after conversion. Hence it is always necessary to carry out a lengthy series of modifications of the network connectivity which improve the realism of the model, mainly by reducing the deviations of interatomic distances and interbond angles from their ideal values (i.e., those in the crystalline phases). The choice arises at once of whether to undertake this process before or after conversion to SiO_2. If the former, the result would be an improved model of a-Si, which could then be converted to a-SiO_2; if the latter, the result would be directly an improved model of a-SiO_2. Our first attempts were along the second path, because we were influenced by the following considerations. In a-Si, a ring of fewer than five atoms forces bond angles deviating at least 49° (for a three-membered ring) or 19° (for a four-membered ring) from the tetrahedral angle, much more than the observed value of about 11°. Hence such rings are not likely to be found frequently in a realistic model of a-Si. On the other hand, insertion of O atoms into these small rings produces rings of six or eight atoms which can exist in configurations that are not highly strained, and might well be present in a-SiO_2. In other words, we did not expect to succeed in modeling a-SiO_2 by trying first to model a-Si. As it turned out, experience has proven otherwise.

The prescription for our first attempts is the following.

1. Place the desired number of Si atoms at random positions in a cubical box.

2. Connect each atom in turn to four of its neighbors, choosing from the nearest remaining atoms that have not yet been fully bonded. Periodic boundary conditions are maintained, and rings of any size above three are allowed; models containing three-membered rings tended to consist of tightly interconnected islands of these rings with only a few external bonds to other islands.

3. Insert an oxygen atom between each pair of Si atoms. A ring of a certain number of Si atoms becomes a ring of the same number of tetrahedra.

4. Move the atoms to positions that minimize an assumed potential energy function and allow the box edge also to take the value that minimizes the potential energy (i.e., that produces the natural density of the model).

5. Change the connections among some subset of atoms, maintaining periodic boundary conditions and tetrahedral coordination, but putting no restrictions on the ring size.

6. Repeat step 4.

7. Compare the tentative new potential energy and density with the previous values. If both have decreased, keep the new configuration and repeat step 5; if either has increased, keep the old configuration and repeat step 5 with some other subset.

When this procedure is followed, changes in the configuration become progressively rarer, and continuing the process becomes unprofitable at some point. The model must then be either discarded as unrealistic, or retained for further examination, if it meets certain standards which we describe later.

As mentioned above, we have found that acceptable models of a-SiO_2 can be produced, contrary to our prejudices, by following a similar procedure except that oxygen atoms are inserted only as the final step, rather than at the outset. In a few cases, the starting network was made from atoms arranged on the sites of a bcc crystal, and rings of fewer than five Si atoms were excluded throughout; these models were the basis of some earlier studies of a-Si.[3]

When the model was treated as a-Si until the very end, its density was fixed at the density of crystalline Si, instead of being allowed to assume its natural value at every stage. A new configuration was accordingly required only to have a lower potential energy, but not to have also a lower natural density than its predecessor. Since the natural density was always higher than that of the crystal, changes which lowered the potential energy in the expanded state would probably also have lowered the natural density, so this procedure is very like the other in this respect, and is computationally faster.

III. POTENTIAL FUNCTION

For models of a-Si we used the Keating potential[4] with the ratio of force constants $\beta/\alpha=0.3$, as found by Keating to best fit the elastic moduli of crystalline Si. For a-SiO_2, we have used a simple extension of the Keating potential, namely,

$$V=\alpha\sum(r_{\mathrm{SiO}}^2-a^2)^2+2\beta\sum(\mathbf{r}_{\mathrm{OSi}}\cdot\mathbf{r}_{\mathrm{OSi}'}-a^2\cos\phi_0)^2+\gamma\sum(r_{\mathrm{OO}}^2-b^2)^2\ . \tag{1}$$

In this expression, the number of terms in the first sum is equal to the number of Si—O bonds ($4N_{\mathrm{Si}}$), the second sum has N_{O} terms, and the third sum has $3N_{\mathrm{O}}$ terms, where N_{Si} and N_{O} are the numbers of Si atoms and O atoms, respectively; $N_{\mathrm{O}}=2N_{\mathrm{Si}}$. The Si—O bond length $a=1.61$ Å was taken from experiment,[5] $b=a\sqrt{8/3}$, and the angle ϕ_0 was assumed to be 142.5°. The computed properties of all examples given in what follows are those in static equilibrium, as judged by the constancy of each of the terms in V after many steps of relaxation. In each step, every atom in turn is moved a distance $\delta\mathbf{r}$ whose x component is proportional to $-(\partial V/\partial x)/(\partial^2 V/\partial x^2)$, with similar formulas for y and z. The equilibrium atomic positions of any example depend only on the ratios β/α and γ/α, and are not very sensitive to these ratios, so that a reasonable approximation suffices during the process of model construction. Narrower limits for these ratios can be found only after completion of the construction.

It was implied in the preceding section that the crudest test of a model is that its density should be close to the observed value,[6] 2.23 g cm^{-3}. Those examples whose properties are described in the following sections gen-

erally had densities not more than 4% greater, and several actually reached slightly lower densities than experimental. Note that the computed density is subject to three times the uncertainty in the assumed bond length a.

Another useful property which depends only on the ratios (β/γ) and (γ/α) is the ratio of the shear modulus μ to the bulk modulus k; this has the value[7] 0.85. For a given model, k is approximately proportional to $(\partial^2 V/\partial\epsilon^2)$ near the minimum of V, where ϵ is the fractional change in box length; this is evaluated automatically in finding the natural density. Because the models are anisotropic, various values of shear modulus are found, depending on the shear mode. We chose for simplicity to perform the three deformations in which one box edge is increased and another decreased equally, and to average the results. The "bulk modulus" is also affected by the anisotropy: strictly we should have allowed the repeating unit to become the parallelepiped whose size and shape result when all six components of the applied stress vanish, and then to apply equal stresses, i.e., a uniform pressure, along each axis. We judged this to be an unwarranted refinement, since the necessary deformations would have been only 1–2 %.

We stated in the Introduction that we rely primarily on diffraction measurements for validation of our models. Fortunately, a-SiO_2 has recently been the subject of a neutron scattering study[5] of great accuracy and range. We also had access somewhat earlier to similar results obtained[8] in this laboratory, and have used these in the graphs shown in the next section. The two sets of data are in remarkable agreement (see Fig. 1; we show here and later the "interference function," $q[S(q)-1]$, first because this is the quantity whose Fourier transform is the RDF, and second, because all deviations of this function from zero are due to structural order). Johnson

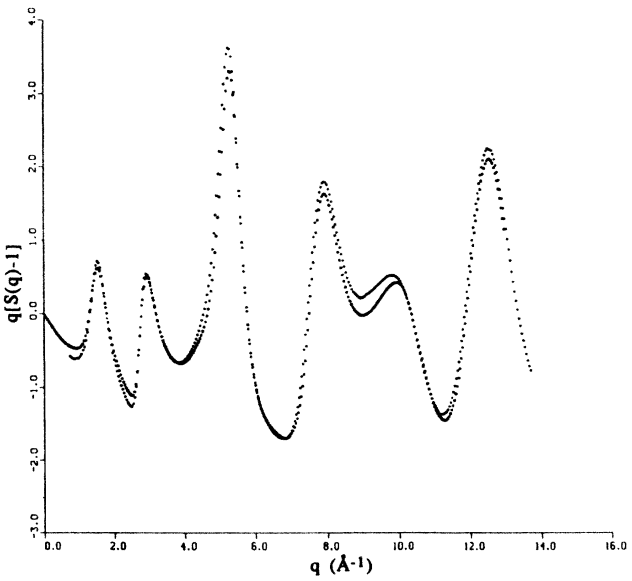

FIG. 1. Comparison of experimental interference functions, $q[S(q)-1]$, data from Ref. 5 (extending to $q=0$), and from Ref. 8.

et al.[5] have derived from their data, particularly at larger momentum transfer, rms values of the variations in the two smallest interatomic distances, namely, 3.1% for the Si—O bond length, and 3.4% for the O—O distance. These values together with the elastic modulus ratio have been used to fix tolerable limits for (β/α) and (γ/α) for each example, and we have then calculated the neutron scattering structure factor for a range of momentum transfer for various pairs $\beta/\alpha, \gamma/\alpha$ within these limits.

IV. STATIC PROPERTIES OF THE MODELS

A. Models treated as SiO_2 from the beginning (type I)

Only three models made this way were judged to have satisfactory densities and variations in interatomic distances; their properties are summarized in Table I, and their neutron scattering structure factors are shown in Figs. 2(a)–2(c), along with the observed[8] factor. The values of β/α and γ/α [Eq. (1)] have been taken to be 0.4 and 0.3, respectively, for all three examples, although somewhat better choices might have been made in individual cases.

Inspection of Fig. 2 shows that, except at the smallest values of momentum transfer q, the calculated structure factors reproduce the observed values very well, both in magnitude and in positions of maxima and minima. However, all three examples exhibit very little intensity at the position of the first observed peak, but large maxima at a small value of q where the real material does not scatter at all. The corresponding real-space distance, $2\pi/q$, while large, is not of course outside the repeat distance of even the 30-atom models. The associated interatomic correlation must be an artifact of the method of model construction whose origins are presently unclear; we return to this question later.

Although many attempts were made to generate other examples of the same sizes or larger, none was successful—the densities achieved were always unacceptably high and the distance distortions too large. Figure 2(d) includes $S(q)$ for the best model with 96 Si atoms. The calculation was not carried further in q because of the poor behavior at small q.

B. Models treated as a-Si from the beginning, and containing no small rings (type II)

The static properties of these examples are shown in Table II, β/α and γ/α having values that gave the "best" overall fit to the density and modulus ratio in each case. These choices were necessarily subjective, on the one hand because there is no obvious limit on what deviations from the experimental values are tolerable, and on the other hand, because the anisotropy of the models introduces uncertainties of 15–20 % in the average modulus ratio. The examples shown differed considerably in their realism as models of a-Si. The calculated structure factors of 5 of these examples are exhibited in Fig. 3. Note that there is no scattering at smaller q than the first observed peak.

TABLE I. Models treated as quartz from start.

Si atoms	Rings 3	4	5	6	7	8	9	Modulus ratio	Cell edge	Dist. dev. (%) Si—O	O—O
30	7	5	3	11	4	0	0	0.83	0.975 20	2.6	3.1
30	8	6	4	6	0	0	0	0.965	0.975 59	3.0	3.0
48	10	10	19	14	4	0	4	0.77	1.009 14	3.9	3.9
									Observed		
								0.85	(1.0)	3.1	3.4

To give some idea of the sensitivity of the density and modulus ratio to the force constant ratios, we show a selection of these data in Table III. A more complete survey of the (β,γ) space did not seem to be worthwhile.

C. Models treated as *a*-Si from the beginning, but containing small rings (types III and IV)

The absence of any scattering by the models of type II at values of momentum transfer below the first observed maximum, in contrast to that by the models of type I, suggested strongly that the numbers of three- and four-membered rings (three or four tetrahedra, thus three or four Si and O each) were features whose influences needed further examination. Models of *a*-Si were constructed therefore in which the rings were no longer required to be larger than five atoms. These models were converted to *a*-SiO_2 when their asymptotic structures seemed nearly to have been attained, even though their angular distortions were usually much larger than would have been acceptable if the purpose had been to model *a*-Si. The resultant models of *a*-SiO_2 (type III), whose static properties are shown in Table IV, were quite realistic on the whole, and their structure factors (Figs. 4 and 5) were generally free of scattering at small q. The starting point in all cases was a 54-atom body-centered cube of Si, with four bonds chosen randomly from first and second neighbors, as in type II. Although the formation of three-membered rings was permitted, the numbers of these rapidly diminished to zero, so they are absent in all of these examples. To illustrate the effects of their presence, Fig. 6 presents the calculated neutron scattering of a single example at a series of stages of its development; it is evident that the scattering generally decreases at the lowest values of q, while rising at the position of the first observed maximum as the number of three-membered rings falls from seven to zero.

The products of the preceding efforts were encouraging enough to warrant attempts to generate larger models. In these, the *a*-Si atoms were initially placed at random in a cubical box, and the density was kept at the density of crystalline silicon subsequently. In earlier

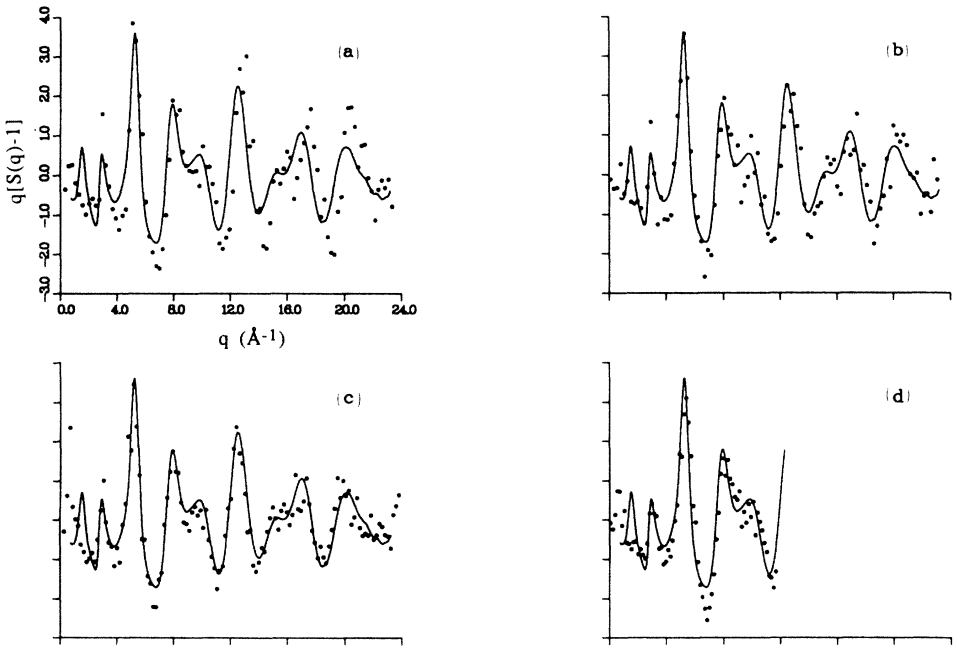

FIG. 2. Interference function calculated for four examples treated as *a*-SiO_2 from the start (type I). The numbers of Si atoms are (a) and (b) 30, (c) 48, (d) 96. Points, simulation; curves, experimental (Ref. 8).

TABLE II. Models with no small rings, 54 Si atoms.

No.	Rings 5	6	7	8	Force constants $\frac{\beta}{\alpha}$	$\frac{\gamma}{\alpha}$	Modulus ratio	Cell edge	Dist. dev. (%) Si—O	O—O
1	29	35	23	1	0.5	0.3	0.93	0.981 15	1.7	2.8
2	31	24	19	6	0.5	0.3	0.89	0.992 35	2.0	3.0
3	36	23	16	0	0.5	0.3	0.89	0.993 25	2.1	3.0
4	30	27	30	0	0.5	0.2	0.83	0.973 62	1.8	4.1
5	29	35	22	0	0.5	0.4	0.91	0.989 12	1.8	2.4
6	27	38	26	2	0.5	0.3	0.74	0.984 83	1.8	2.5
							0.85	Observed (1.0)	3.1	3.4

work, the search for connectivity changes that were most likely to lower the strain energy usually began on close, unbonded Si pairs. In the present series, the search began on the Si atoms whose individual contributions to the strain energy were the highest. This tactic was a natural one for computations using a vector computer, like the CRAY, since the individual contributions were routinely computed and stored anyway. It also appealed on physical grounds, in comparison to searches which emphasize only one aspect of the strain, such as bond distortions alone, or angle distortions alone. A number of examples containing 108 Si atoms were constructed and converted to a-SiO_2 (type IV). The static properties are in Table V, and the neutron diffraction patterns in Figs. 7 and 8.

V. DISCUSSION OF THE RESULTS

The most obvious distinction between models having various topologies derives from their structure factors in the region of small momentum transfer. The presence of numerous rings joining three tetrahedra, as in those of type I, leads to a displacement of the first maximum in $S(q)$ to values much smaller than are observed. When three-membered rings are absent, the first clear maximum occurs at the right value of q, but only if the number of four-membered rings is not too large. When there is more than about one four-membered ring per ten Si atoms, the intensity of the first maximum falls below the experimental value, while the intensity at smaller q rises above the experimental. It does not seem possible to correlate these trends with the numbers of larger rings without constructing many more examples, particularly with 108 atoms or more, to allow eight- and nine-membered rings.

For models whose small-q behavior is satisfactory, it can be seen from Figs. 3, 4, and 7 that the other features of $S(q)$ are also reproduced very well. When the natural density of the model is too high, the interatomic distances are too small, and the calculated maxima there-

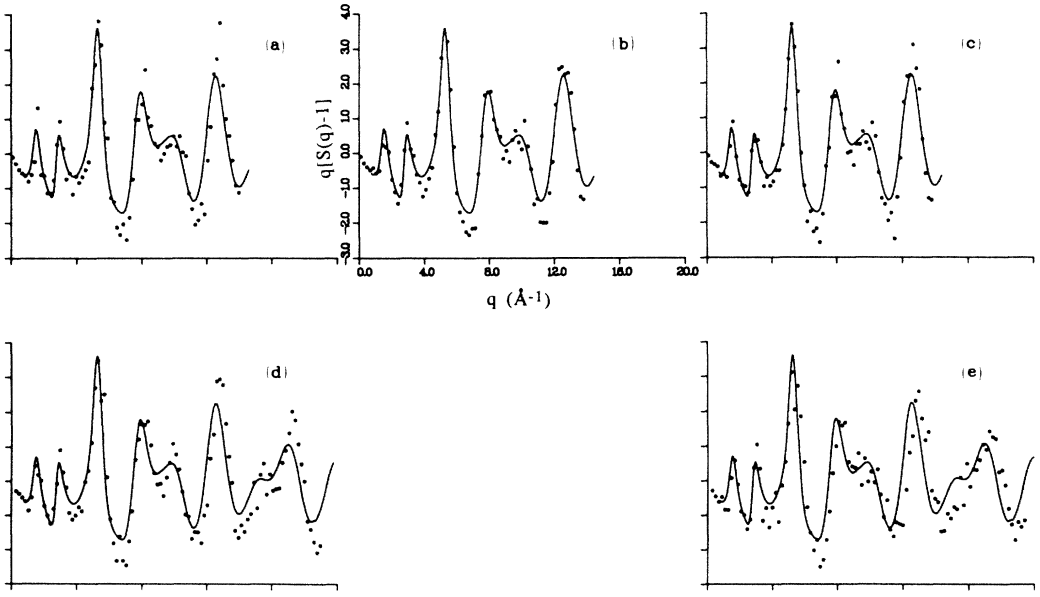

FIG. 3. Interference function calculated for examples treated as a-Si from the start (type II) in the order of Table II. Points, simulation; curves, experimental (Ref. 8). Repeating unit held 54 Si atoms.

TABLE III. Effect of varying force constants on cell size and modulus ratios for examples 1–5.

		No. 1		No. 2		No. 3		No. 4		No. 5	
β/α	γ/α	Cell edge	μ/k	Cell edge	μ/k	Cell edge	μ/k	Cell edge	μ/k	Cell edge	μ/k
0.3	0.4	0.9717	1.33			0.9877	1.14			0.9834	1.16
0.4	0.3	0.9734	1.35	0.9901	0.97	0.9910	0.95	0.9647	1.16	0.9890	0.89
0.5	0.2	0.9842	0.75					0.9736	0.83		
0.5	0.3	0.9812	0.93	0.9924	0.89	0.9933	0.89				
0.5	0.4	0.9782	1.05			0.9947	0.73	0.9630	1.20	0.9892	0.91

TABLE IV. Models with four-membered rings, 54 Si atoms.

	Rings						Force constants		Modulus ratio	Cell edge	Dist. dev. (%) Si—O	O—O
No.	4	5	6	7	8	9						
1	3	29	28	27	0	0	0.5	0.3	0.89	0.991 14	1.9	3.0
2	9	22	28	26	6	0	0.5	0.3	0.90	1.007 35	2.0	3.1
3	6	28	27	13	3	2	0.5	0.3	0.84	1.011 63	1.5	2.2
4	6	25	28	22	6	1	0.5	0.3	0.89	0.992 30	2.0	3.0
5	5	27	25	25	4	1	0.4	0.3	0.73	1.008 32	1.4	2.2
										Observed		
									0.85	(1.0)	3.1	3.4

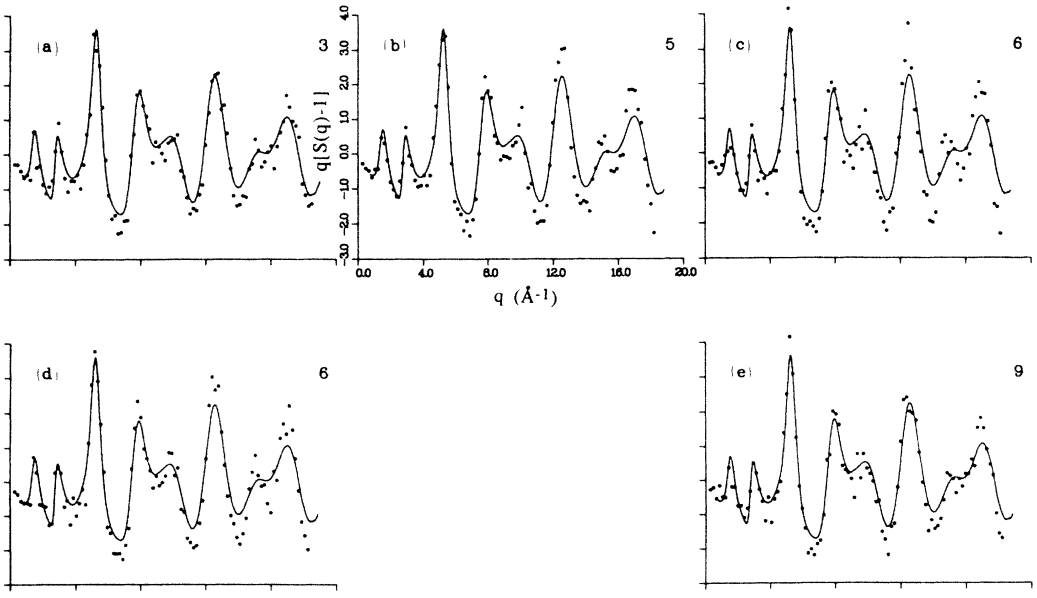

FIG. 4. Interference function calculated for examples treated as *a*-Si from the start with no restrictions on the ring sizes (type III) in the order of Table IV. Points, simulation; curves, experimental (Ref. 8). Repeating unit held 54 Si atoms. Labels are the numbers of four-membered rings.

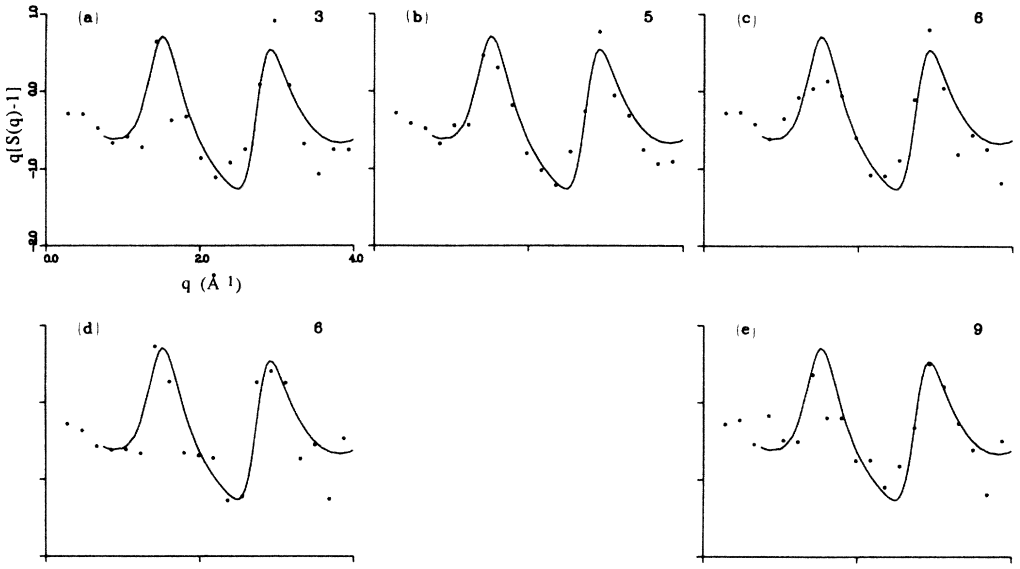

FIG. 5. Same examples as Fig. 4, small-q data on an expanded scale.

fore occur at somewhat too large q. The deviations of the Si—O and O—O distances for models of types II–IV are always smaller than observed, i.e., the models are insufficiently disordered. This has the effect of making the calculated maxima higher than observed, but it should be noted that the experimental data were taken at room temperature. The observed maxima have therefore been attenuated by a Debye-Waller factor, which, if its value were known, could be removed, bringing the static models into even closer agreement with observations. Alternatively, if a reliable vibrational spectrum could be calculated (as we intend to do), the room-temperature scattering by vibrating models could also be calculated.

The force-constant ratios β/α and γ/α have been chosen in some cases to fit the elastic modulus ratio and density (type II) while in most of the other cases (types III and IV) an overall fit has been achieved by a single choice. For reasons already stated, it does not seem possible to determine the force constants with great precision. Moreover, a purely valence-force law, although it may be adequate for studies of the static properties, is certainly not so for dynamical properties, since the atoms are charged.

VI. ORIGIN OF THE SMALL-q SCATTERING

Much reliance has been placed on the calculated structure factor in the neighborhood of the first observed maximum as a means of validating the models. As we have stated, the presence of any three-membered rings or of four-membered rings seems to be correlated with scattering at q in the range 0.5–0.7 A^{-1}, and in extreme cases, absence of scattering at the observed position of the first maximum. It is peculiar that a correlation

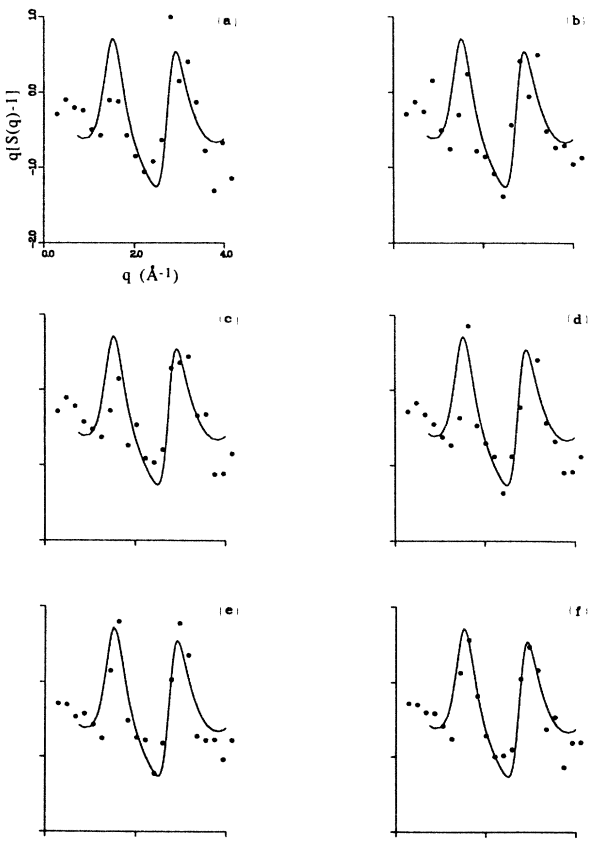

FIG. 6. Interference function calculated for a single example at various stages. Repeating unit held 54 Si atoms. Numbers of three- and four-membered rings: (a) (7,8), (b) (2,10), (c) (2.9), (d) (0,8), (e) (0,7), (f) (0,8) (final state).

TABLE V. Models with 108 Si atoms.

No.	Rings 4	5	6	7	8	9	Modulus ratio	Cell edge	Dist. dev. (%) Si—O	O—O
1	11	56	61	40	23	3	0.82	0.998 10	1.8	2.7
2	18	54	55	40	13	11	0.85	1.003 28	1.9	2.9
3	9	54	62	58	20	1	0.96	0.996 69	1.4	2.0
4	12	52	57	53	21	9	0.95	0.998 65	1.6	2.6
5	13	57	62	30	24	9	0.90	1.006 12	1.7	2.8
6	15	53	66	37	11	3	0.81	1.002 23	1.9	2.7
								Observed		
							0.85	(1.0)	3.1	3.4

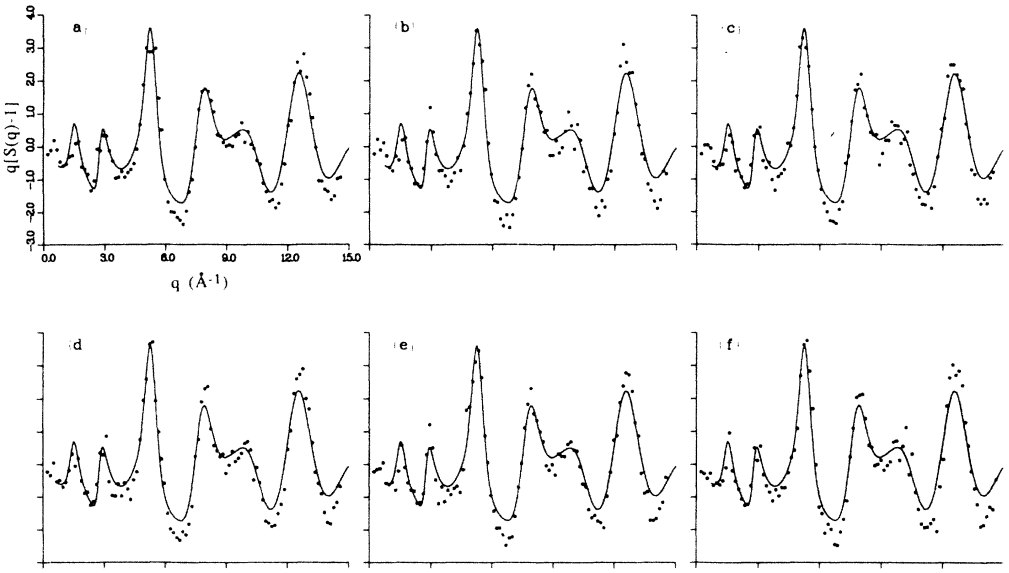

FIG. 7. Interference function calculated for examples treated as *a*-Si from the start (type IV). Repeating unit held 108 Si atoms. Numbers of four-membered rings: (a) 18, (b) 15, (c) 13, (d) 12, (e) 11, (f) 9.

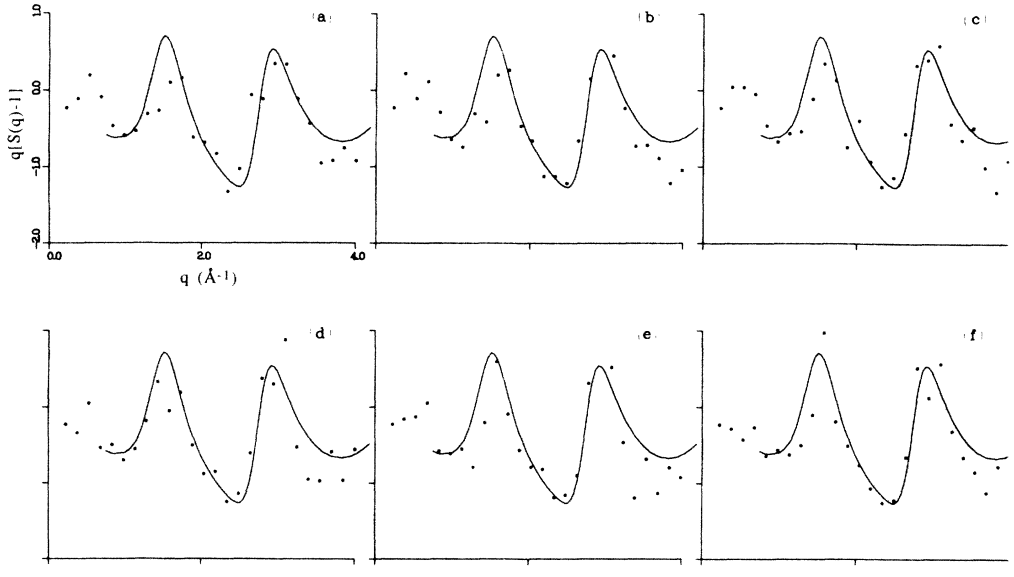

FIG. 8. Same examples as Fig. 7, small-*q* data on an expanded scale.

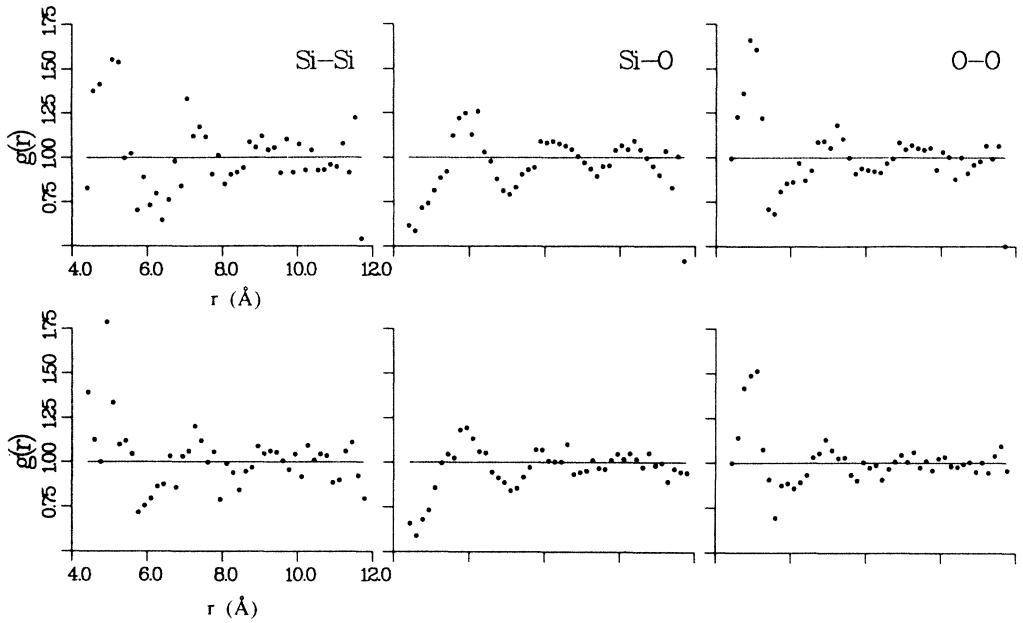

FIG. 9. Radial distribution functions of two examples with maximal difference in numbers of four-membered rings. Upper figures, nine rings (no. 3 in Table V); lower figures, 18 rings (no. 2 in Table V). Horizontal lines are drawn at $g = 1.0$ for each set.

should exist between a scattering feature at small q, therefore large distance, and a structural element at moderate distance, at any rate smaller than distances typical of larger rings. If such a correlation exists, it ought to be apparent in the real-space radial distribution function, $g(r)$, at distances near $2\pi/0.6$, about 10 Å. Unfortunately, this is a region that is hard to examine with models of the present size. In sampling $g(r)$, when r exceeds half the size of the unit cell, d, more and more pairs are encountered whose actual distance is less than $d/2$ because of the periodic boundary conditions. The sampling must then be restricted to volume elements bounded by only parts of the full spherical surface, and this part vanishes exactly at $\frac{1}{2}\sqrt{3}d$. The statistical error in g thus increases for $d/2 \leq r \leq \frac{1}{2}\sqrt{3}d$. Reciprocally, the structure factor cannot be computed for $q < 2\pi/d$, and its statistical error is large for q only slightly greater; i.e., only a few Bragg reflections contribute to $S(q)$ near this lower limit.

We have nevertheless computed the three functions g_{SiSi}, g_{SiO}, and g_{OO} for two examples containing 108 Si atoms, denoted by nos. 2 and 3 in Table V; these examples have the fewest and the most four-membered rings of their class, and should therefore differ most in g. The distance extended to $d/\sqrt{2}$ in r, at which distance only about 3% of the pairs remained unsampled. The results, in Fig. 9, show, if anything, *less* structure at large r for the example having the larger scattering at small q, and are of no help in clarifying the observations. Moreover, the maximum in $S(q)$ appears in all three of the partial structure factors (not shown here), so that the structural correlation responsible is common to all types of pairs, as might be expected at an interatomic separation that is much larger than the Si—O bond length.

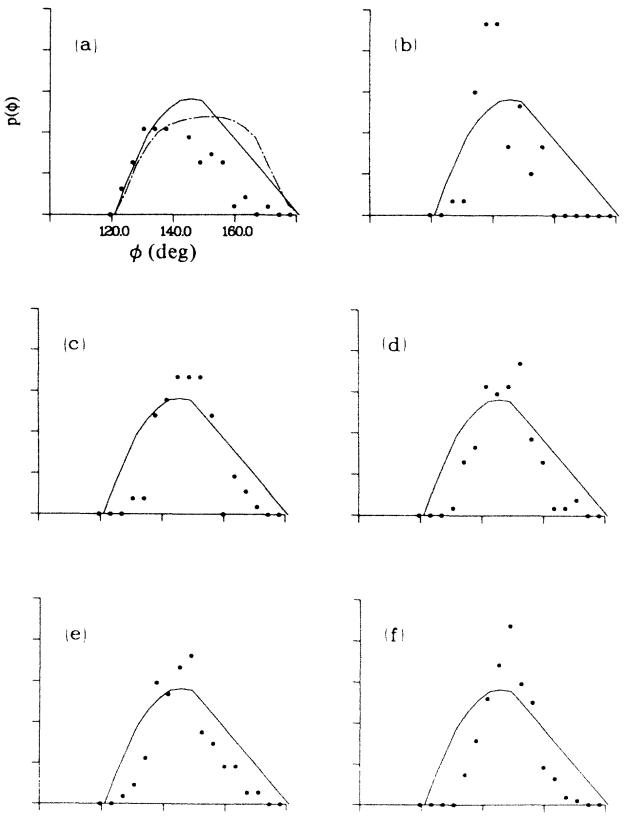

FIG. 10. Intertetrahedral angle distribution. Solid line, Mozzi and Warren (Ref. 9); dashed line, Dupree and Pettifer (Ref. 10). Points, simulation: (a) 48 Si, Table I, no. 3; (b) 30 Si, Table I, no. 2; (c) 54 Si, Table IV, no. 4; (d) 54 Si, Table II, no. 3; (e) 108 Si, Table V, no. 2; and (f) 108 Si, Table V, no. 3.

VII. INTERTETRAHEDRAL ANGLE AND DIHEDRAL ANGLE DISTRIBUTIONS

The angles between the O—Si bonds at a common oxygen atom should tend, according to the second term in Eq. (1), to be close to ϕ_0. In actuality, these angles are broadly distributed, both in the real material and in our models. Representative values are shown in Fig. 10, for comparison with those measured by x-ray diffraction[9] and by a nuclear magnetic resonance technique.[10] The models all show much narrower distributions than either of the experimental results, but are more like that of Mozzi and Warren.[9] Further, the models of type I differ more from Mozzi and Warren's result than do those of the other types, confirming the view that the latter are more realistic.

The orientation of a tetrahedron with respect to nearby atoms must also be specified by the value of an angle of rotation about one of its Si—O axes. One such definition is the dihedral angle between two planes, one containing an oxygen atom and its two silicon neighbors, the other containing that oxygen atom, one of the Si atoms, and another O atom in the same tetrahedron. This is the definition adopted by Gaskell and Tarrant[1] in their study of the Bell-Dean model of a-SiO_2, and is apparently that used by Galeener[11] in his analysis of the dihedral angle distribution.

The distribution of dihedral angles ψ has been calculated for the examples of types II, III, and IV, and is plotted in Figs. 11, 12, and 13, respectively. Within the rather large scatter imposed by the number of angles (three times the number of Si atoms) these figures generally show no deviations from randomness.

Although the dihedral angle distribution is not directly measurable, it does affect the distribution of Si—O second-neighbor distances, shown in Figs. 14 and 15 for the examples of types II and IV, respectively. As discussed for their models by Evans *et al.*,[2] this function typically has two maxima, a narrow one at 4.2 Å coming from pairs for which ψ is near 180°, and a much broader one near 3.5 Å, for ψ near 0°. If the SiO_4 tetrahedra were perfect, these maxima could be attributed to distributions of ψ which could be called "staggered" and "eclipsed," and a greater prominence of the peak at

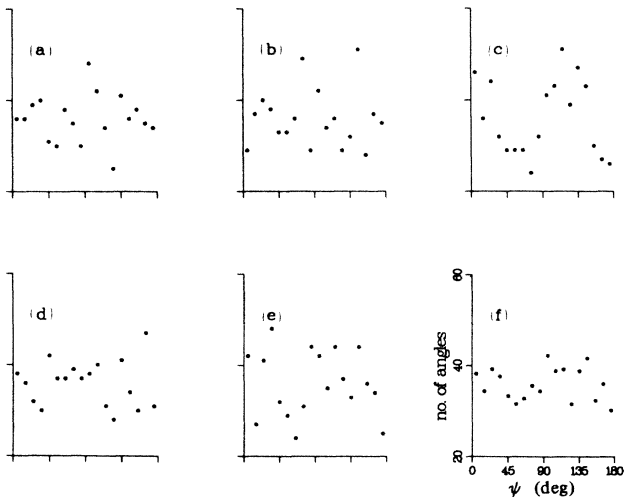

FIG. 11. Dihedral angle distribution, models of type II. (a)–(e) Examples in order of Table II, (f) average.

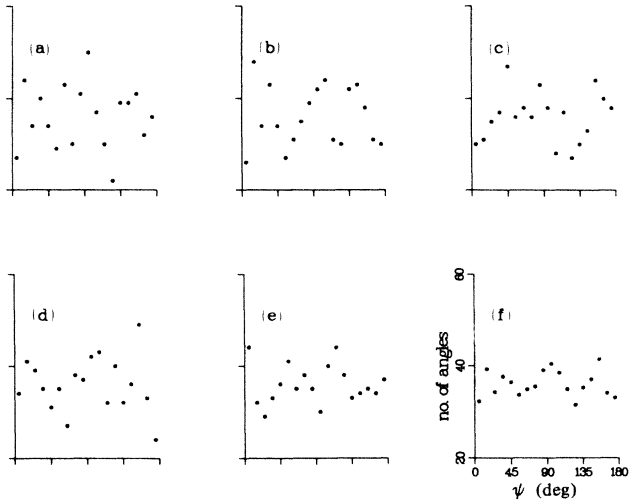

FIG. 12. Dihedral angle distribution, models of type III. (a)–(e) Examples in order of Table IV, (f) average.

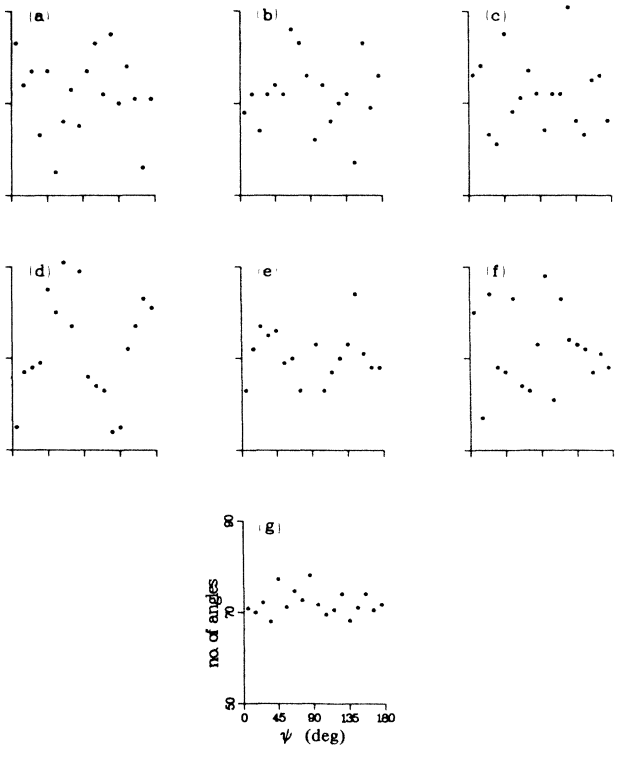

FIG. 13. Dihedral angle distribution, models of type IV. (a)–(f) Examples in order of Table V, (g) average.

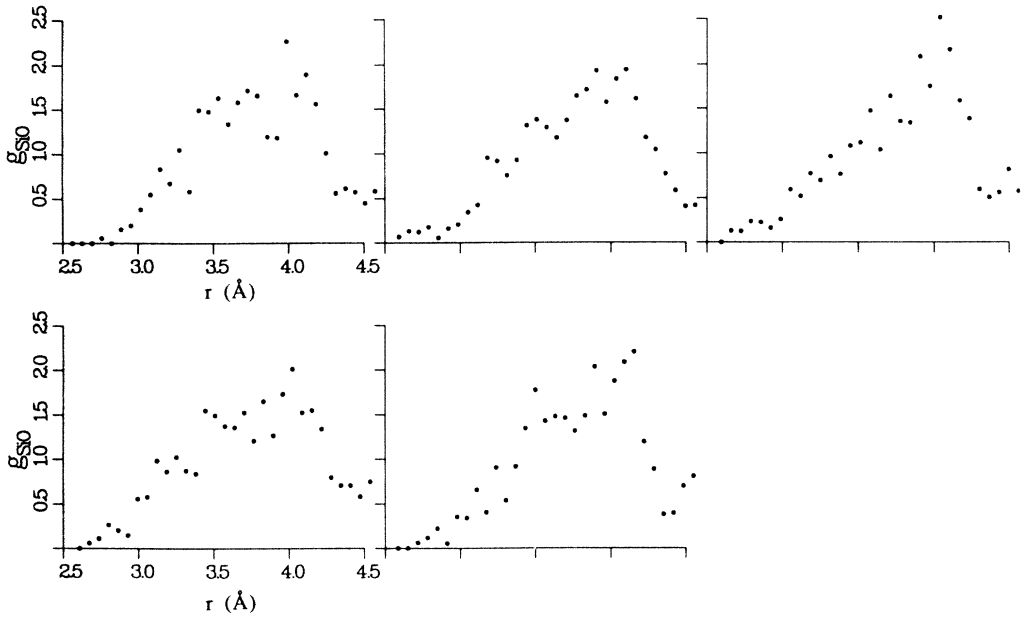

FIG. 14. Radial distribution function for pairs of unlike atoms, examples of type II in the order of Table II.

smaller distance could be attributed to a tendency toward the eclipsed form (contrary to the statement by Evans *et al.*). The experimental radial distribution function[12] has less structure near 3.5 Å than any of the models treated by Evans *et al.*, suggesting that staggered arrangements are favored in the real material. The Si—O radial distribution functions of Figs. 13 and 14 exhibit the 3.5-Å maximum only rather weakly, but this cannot be so clearly connected with staggered ψ distributions, as the latter are generally random. In fact, the 3.5-Å peak is least evident in the example whose ψ distribution is most clearly eclipsed (type II, no. 3). We conclude that a proper analysis must take into account other correlations, such as that between bond lengths and bond angles, especially that between the Si—O—Si angle and adjacent dihedral angles.

The absence of significant deviations of dihedral angles from a random distribution for the present models is just what we would expect, since the potential function does not depend explicitly on the dihedral angle. If nonrandom distributions have developed, as shown occasionally in Figs. 10 and 12, this must have occurred as

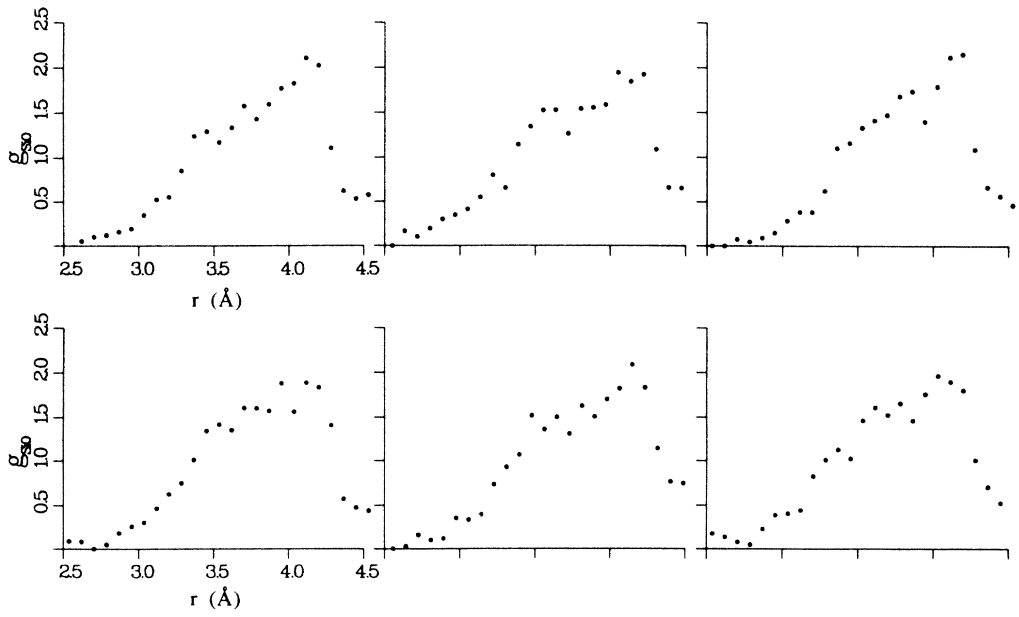

FIG. 15. Radial distribution function for pairs of unlike atoms, examples of type IV in the order of Table V.

a consequence of the final topology, especially when one recalls that all of the models of types II–IV were treated as *a*-Si during the process which generated that topology.

VIII. CONCLUSIONS

To the preceding discussion, which has been directed to the details of the topology of our models, we should add the general statement that our results confirm the continuous random network structure. It may also be claimed that our procedure has exhausted the information content of the experimental neutron-diffraction data. Random network models differing from ours in topology, or models of other types, if they conformed equally well to the diffraction data, could equally claim legitimacy. However, it seems likely that substantial progress in modeling could be achieved only by making more use of the values of $S(q)$ at its extrema, which requires that the nonzero temperature effects be included.

Our potential function has the virtues of simplicity and convenience, but as noted earlier, its validity extends at most to determining the static structure and a few bulk properties. The Si—O bonds must be appreciably ionic, and consequently long-range forces must also play a role in these properties and to an even greater extent in the vibrational spectrum. A logical approach to a more comprehensive investigation could use the structures of our most realistic examples as conditions on the parameters of a potential function which includes Coulombic terms. Additional conditions would be provided by the observed infrared absorption spectrum and neutron inelastic scattering. We plan to calculate the vibrational spectra of these models. Finally, in justification of having presented these findings at such length, we want to stress the variability of structural models of glasses, and the dangers of basing general conclusions on single examples. Our procedures are far freer of subjective influences than is usual in this field, and yet we have seen how much the properties of one example of a given type may differ from those of another constructed according to the same rules.

ACKNOWLEDGMENTS

We are grateful to David Price for providing the neutron scattering data in digital form before publication. Extensive computations were carried out on the Energy Research Cray X-MP and Cray 2 at the Magnetic Fusion Energy Computing Center. S.R. would like to thank Beloit College, Beloit, Wisconsin for financial support.

---

*Permanent address: Allegheny College, Meadville, PA 16335.

[1]P. H. Gaskell and I. D. Tarrant, Philos. Mag. B **42**, 265 (1980).

[2]K. M. Evans, P. H. Gaskell, and C. M. M. Nex, in *Structure of Non-Crystalline Materials,* edited by P. H. Gaskell, J. M. Parker, and E. A. Davis (Taylor and Francis, London, 1982), p. 426.

[3]L. Guttman, W. Y. Ching, and J. Rath, Phys. Rev. Lett. **44**, 1513 (1980).

[4]P. Keating, Phys. Rev. **145**, 637 (1966).

[5]A. V. Johnson, A. C. Wright, and R. N. Sinclair, J. Non-Cryst. Solids **58**, 109 (1983).

[6]G. K. White and J. A. Birch, Phys. Chem. Glasses **6**, 85 (1986).

[7]*American Institute of Physics Handbook,* 2nd ed. (McGraw-Hill, New York, 1963), pp. 3–88.

[8]M. Arai and D. L. Price (unpublished).

[9]R. L. Mozzi and B. E. Warren, J. Appl. Crystallogr. **2**, 164 (1969).

[10]E. Dupree and R. F. Pettifer, Nature (London) **308**, 523 (1984).

[11]F. L. Galeener, J. Non-Cryst. Solids **75**, 399 (1985).

[12]A. C. Wright and R. N. Sinclair, in *Physics of SiO_2 and Its Interfaces,* edited by S. T. Pantelides (Pergamon, New York, 1978), p. 133.